Gawalapu (2012) Biotechnology International 5(2): 28-51

www.bti.org.in
ISSN 0974-1453

Research paper

COMPUTATIONAL ESTIMATION OF THE ENERGY REQUIREMENTS FOR CONFORMATIONAL TRANSITIONS IN SKELETAL MUSCLE MYOSIN

Ravi K.Gawalapu
Jackson Heart Study, Jackson, MS

Corresponding author: ravi_kumar.gawalapu@jsums.edu

ABSTRACT: In order to determine the energy consumption during transitions between critical conformational states of myosin S1, molecular mechanics and dynamics simulations were applied to native myosin S1 structure. Dynamics simulations on the myosin S1 motor domain indicated that significant flexibility was present throughout the molecular model. The conformational transition is induced using a spring constant of 16.7 N/m. A simulated force-distance curve is calculated based on the difference between the actual distance and target distance after successive energy minimizations and the area under the force distance plot is determined. Analysis of different conformational states provided new insights into energy consumption in myosin S1 and molecular level details of the complex internal interactions of myosin. Cross linking reactive cysteines SH1 and SH2 with nucleotide binding site closed/open are consistent with experimental studies. Energy consumption is maximum when SH1 SH2 reactive cysteines are crosslinked with nucleotide binding site open.

KEYWORDS: Myosin, Molecular motors, Energy minimization, Molecular dynamic simulations, Conformations, RMSD(Root mean square deviations).

INTRODUCTION

Molecular motors are enzymes which during the course of their catalytic cycle, can generate force and perform work, in moving along a track against a constant force. Even after decades of study, the relationship between a motor's enzymatic mechanisms and its mechanism for force and work production is uncertain. A central goal into the mechanism of muscle contraction is to understand the structural basis of the power stroke of the myosin cross-bridge. In multi-subunit proteins like myosin, the rearrangement of the packing of subunits and the conformational change is

responsible for function. Such an understanding requires knowledge of the structural transitions that myosin makes while bound to the actin filament. Since, the crystal structures of the actomyosin complex are missing and the available crystal structures represent only a few steps of the cycle and obtaining atomic structures that represent the motors bound to their filament has been difficult. It has not been possible to know the effect of actin binding to myosin on itshead structure in general and, specifically on the conformationalchange of the lever arm occurring during the working strokeof cycling cross bridges. A crystal structure will also limit the interpretation, as a crystal structure is a static picture of a single conformation of a protein, obtained in the presence of crystal contact packing forces and undernon-physiological conditions. It is therefore necessary to supplement the insights obtainedfrom x-ray crystallography with non-static analyses. In this regard, molecular dynamics simulations offer us an extremely powerfultool for analyzing the structural, mechanistic, and energeticproperties of biomolecules (Todd et al. 2002). Large-scale conformational transitions driven by a distant chemical event, such as ligand binding, is the hallmark of many allosteric systems (Roberts, etal.1994). In this regard, molecular motors are striking examples (Vale RDet al.2000 J.) in which the hydrolysis of ATP induces large-scale structural rearrangements in regions far from the nucleotide binding site. Since the function of molecular motors is likely dependent on a tight coupling between the chemical and the mechanical events, understanding the mechanism of such mechanochemical coupling at the molecular level has been an actively pursued objective in modern biophysics.

X-ray diffraction was the first source of information about muscle structure at the molecular level (Huxley,1996). Duringthe last two decades, this method was significantly improved byusing bright synchrotron radiation sources and modern 2D detectors(Harford and Squire, 1997), so that its spatial (Huxley et al.1994; Wakabayashi et al.1994)and time(Dobbieet al.1998) resolutions are now significantly higherthan provided by other methods used for structural studies ofmuscle. The present study represents to examine energetic

properties concerning the conformational transitions in skeletal myosin S1. The assumption that this energy is used to generate force and produce work has been a major tenet of many theoretical models of the actomyosin interaction, (Huxley, 1957; Eisenberg et al,1980; Pate and Cooke, 1989) but this assumption has not been previously verified in a quantitative manner. Based on energy consumption among different myosin families one can understand the difference in their function. The success of this method lends support to the critical roles of collective low-frequency motions in facilitating biomolecular functions.

In order toelucidate the detailed mechanism of a given enzyme, it is necessaryto estimate quantitatively the energy required for domain movement.For the last 2 decades, molecular dynamic calculations have beenused to predict the domain movement of enzymes (Pugmire, 1998; McCammon, 1983). Recentstudies indicate that single molecule measurements may also beuseful in determining the energy required for domain fluctuation(Radmacher, et al. 1994; Mehta, Rief, Spudich, Smith and Simmons, 1999). Despite these trials, it has proven difficultto confirm quantitatively the free energy required for domainmovement of an enzyme. Many experiments with a number of proteins like myosin haverevealed domain movement in aqueous solution by using substrateanalogs or have directly revealed movement by x-ray crystallography (Wakabayashi etal.1999). Computational simulation is a valuable tool assisting in studies of complicated 3D molecular objects especially when direct observation is technically impossible to understand relation between energy requirements and structural changes. In this paper, we estimated the energy required for critical conformational states of myosin S1, to understand relation between energy requirements and structural changes. The conformational transition is induced using a spring constant of 16.7 N/m. A simulated force-distance curve is calculated based on the difference between the actual distance and target distance after successive energy minimizations and the area under the force distance plot is determined. Although the final details of the myosin motor mechanism await actin–myosin co-crystals, the fact that myosin can

populate multiple states in the absence of actin has allowed great insight into the mechanism of molecular motors of the myosin superfamily.

MATERIALS AND METHODS

Conformational searching, stochastic dynamics simulations, and energy minimizations are performed using the Macromodel software (version 8; Schrodinger,Inc). The atomic model of chicken skeletal myosin S1 (Raymentet al,1993a) was reconstructed with the missing surface loops by individual local applications in shells of 1 nm of the Macromodel LOOP algorithm (100 steps) followed by a seeded mixed large scale low mode and Monte Carlo (1000 steps) conformation searches to identify the lowest energy structures. The myosin heavy chain is truncated to residue 792 to leave only the motor domain. Energy minimization and subsequent simulations of the entire modified chicken skeletal myosin S1 is performed using the AMBER* force field and a generalized Born / solvation area model as previously (Root et al.1999).

Procedure for 50 kDa cleft opening/closing

Atomic model of native myosin S1 is energy minimized as previously(Gawalapuet al.2006). To the native energy minimized structure, eleven pairs of harmonic constraints are applied evenly between the upper and lower subdomains around the cleft. These constraints were selected such that these residues were not part of any loop or actin binding interface. Each distance constraint is incremented/ decremented by 0.1 nm followed by energy minimization. The resultant structure is again energetically minimized for a maximum of 5000 iterations with a convergence threshold of 1. This process is repeated for 12 times and then the resultant structure is dynamically simulated for 100 ps with the maximum number of iterations being 500 and a convergence threshold of 0.05. Stochastic dynamic simulations allow the atomic model to relax without the constraints of crystal lattice or force restraints.

Procedure for SH1-SH2 crosslinking

For SH1-SH2 crosslinking distance constraint is applied to CYS 697 and CYS 707 to the energy minimized native myosin S1 structure. The two reactive cysteines are separated by a

distance of 2 nm. The two cysteines are pulled closer by 0.1 nm during each energy minimization cycle. Force constraints with a spring constant of 16.7 N/m were used to crosslink the two cysteinesby changing the target distance at 0.1 nm decrements followed by energy minimization. This process is continued till the two cysteines are at a distance of 0.3 nm. This entire process takes 34 energy minimization cycles. The final energy minimized structure of the cross linked cysteines is compared to the energy minimized structure of native myosin S1. The structure obtained after 100 ps of stochastic dynamic simulations is compared to the native myosin S1 after 100 ps of stochastic dynamic simulations.

Procedure for opening nucleotide binding site

For opening ATP binding site distance constraint is applied to SER 180 and SER 320 of the energy minimized native myosin S1 structure. The two serines are separated by a distance of 1.5 nm and are a part of the phosphate binding site. The two serines are pulled apart by 0.1 nm during each energy minimization cycle. Force constraints with a spring constant of 16.7 N/m were used to open the nucleotide binding site by incrementing the target distance at 0.1 nm followed by energy minimization. This process is continued till the two serines are separated to a distance of 2.5 nm from 1.5 nm. This entire process takes around 17 energy minimization cycles. Stochastic dynamic simulations are done for 100 ps to the final structure with the without any constraints attached to the two serines. The final energy minimized structure of the nucleotide opened structure is compared to the energy minimized structure of native myosin S1. The structure obtained after 100 ps of stochastic dynamic simulations is compared to the native myosin S1 after 100 ps of stochastic dynamic simulations.

Procedure for crosslinking SH1 SH2 with nucleotide binding site open

The structure obtained from 100 ps of stochastic dynamic simulations with constraints attached to the two serines (nucleotide binding site) is taken as the starting structure for crosslinking SH1-SH2. To this structure the reactive cysteines are crosslinked. Distance constraints are applied to CYS 697 and CYS 707 which are separated by a

distance of ~2 nm. The two cysteines are pulled closer by 0.1nm during each energy minimization cycle and the two serines are also constrained and kept at a distance of 2.5 nm so that the nucleotide binding site is not closed. This process is continued till the two cysteines get to a distance of 0.3 nm. This entire process takes 31 energy minimization cycles. Stochastic dynamic simulations are done for 100 ps to the final structure with the two cysteines at 0.3 nm and the two serines at 2.5 nm with constraints attached to the two cysteines and the two serines during simulation. Stochastic dynamic simulations are also done without any constraints to the two cysteines and the two serines. The final energy minimized structure is compared to the energy minimized structure of native myosin S1 obtained after 100 ps of simulation. The structure obtained from stochastic dynamics simulations is compared to the simulated structure of native myosin S1 obtained from 200 ps of stochastic dynamics simulations.

Procedure for opening/closing the 50 kDa cleft after crosslinking SH1-SH2

The structure obtained from 100 ps of stochastic dynamics simulations with the two cysteines cross linked and at 0.3 nm with constraints attached to the two cysteines during simulation is taken as the starting structure. To this structure distance constraints were applied around the 50 kDa cleft to open/close the 50 kDa cleft. The distance constraints are incremented/decremented by 0.1nm during each energy minimization cycle and also the two cysteines are constrained and are kept at a distance of 0.3 nm. This process is continued till the 50 kDa cleft is opened/closed. This entire process takes 12 energy minimization cycles. Stochastic dynamic simulations are done for 100 ps to the final structure with the two cysteines at 0.3 nm with constraints attached to the two cysteines during simulations. The final energy minimized structure is compared to the energy minimized structure of native myosin S1 after 100 ps of simulation. The structure obtained after 100 ps of stochastic dynamic simulations is compared to the native myosin S1 after 200 ps of stochastic dynamics simulations.

Procedure for opening/closing the 50 kDa cleft with nucleotide binding site opened

The structure obtained from 100 ps of stochastic dynamics simulations with constraintsattached to the two serines and separated by 2.5 nm is taken as a starting structure foropening/closing the 50 kDa cleft with nucleotide binding site opened. To this structuredistance constraints are applied around the 50 kDa cleft to close the 50 kDa cleft. Thedistance constraints are incremented/decremented by 0.1nm during each energy minimization cycle and also the two serines are constrained and are kept at a distance of2.5 nm. This process is continued until the 50 kDa cleft is opened/closed. This entireprocess takes 12 energy minimization cycles. Stochastic dynamic simulations are donefor 100 ps to the final structure with the two serines at 0.3 nm with constraints attached tothe two serines during simulations. The final energy minimized structure is compared tothe energy minimized structure of native myosin S1 after 100 ps of simulation. Thestructure obtained from 100 ps of molecular dynamics simulations is compared to thenative myosin S1 after 200 ps of molecular dynamics.

Procedure for opening/closing the 50 kDa cleft with crosslinked SH1 SH2 and nucleotide binding site opened

The structure obtained from stochastic dynamic simulations for 100 ps with the twocysteines at 0.3 nm and the two serines at 2.5 nm with constraints attached to the twocysteines and the two serines during simulation is taken as the starting structure toopen/close the 50 kDa cleft. To this structure distance constraints were applied around the50 kDa cleft to open/close the 50 kDa cleft. The distance constraints are incremented/decremented by 0.1 nm during each energy minimization cycle and alsoduring the energy minimization the two serines are constrained and are kept at a distanceof 2.5 nm and the two cysteines are also constrained and kept at a distance of 0.3 nm.This process is continued until the 50 kDa cleft is opened/closed. This entire processtakes 12 energy minimization cycles. Stochastic dynamic simulations are done for 100ps to the final structure with constraints attached to the two serines and the

two cysteinesduring simulations. The final energy minimized structure is compared to the energyminimized structure of native myosin S1 after 200ps of simulation. The structureobtained from 100 ps of stochastic dynamic simulations is compared to the nativemyosin S1 after 300 ps of stochastic dynamic simulations.

RESULTS AND DISCUSSION

Simulations near the converter region

The SH1 (Cys-707) and SH2 (Cys-697) groups are the two most reactive cysteines on the myosin head (S1). Crosslinking SH1-SH2 with the nucleotide binding site closed does not show any changes in the structure (Fig 1 A). A force constraint was applied between these residues to computationally crosslink them in the atomic model. The residues are located on the opposite side of a short helix in the catalytic domain of the myosin head and are separated from one another by ~20 Å. (Rayment, et al.1993b). The firstevidence of the mobility of this helix came from cross-linkingexperiments. The mechanism by which this helix is involved in the force generation cycle is still unknown. Crosslinking the reactive cysteines induced movements that correlated with modest changes throughout the motor domain particularly in the normally flexible regions identified by the dynamics simulations (Fig 1 B). The structure does not get back to original RMSD during relaxation, which suggests that the crosslinking of cysteinescauses a change in flexibility. This is also seen during many cysteine crosslinking experiments like loss of ATP ase activity inactivation of motility and trapping of nucleotide (Reisleret al.1992). The strut region seems to be the most rigid in the motor domain as it does not get perturbed and has one of the lowest RMSD. The force-distance plot shows that the crosslinking of reactive cysteines requires substantial force as the structure has to undergo some major barriers like the unraveling of the alpha-helix that separates the two residues and so the force rises during few stages and then drops (Fig 1 C). Crosslinking caused little change in the helix leading to the lever arm. If conformational changes from crosslinking were directly involved in lever arm movement, then the computational crosslinking should have affected this helix. Indirect positioning

of the lever arm through light chain interactions with the converter region and the SH3 domain seem more consistent with the simulations. It has been suggested that the light chain binding domain is required to see the expected conformational change at the fulcrum point.

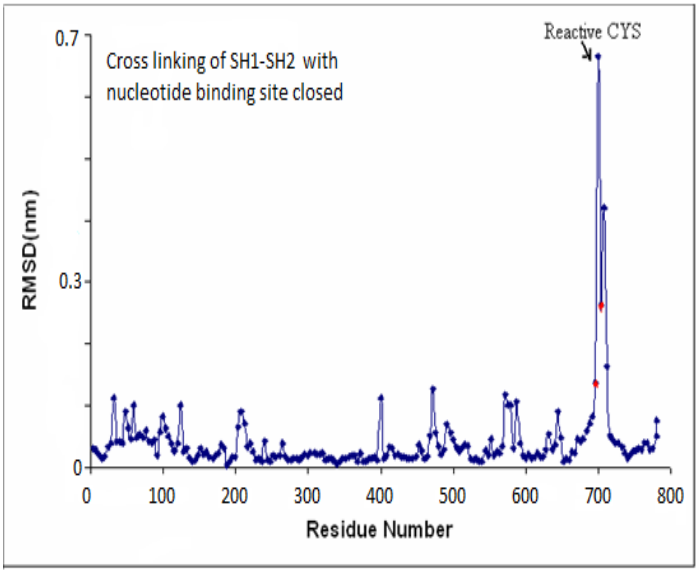

Fig. 1A: Structural changes associated with crosslinking of the reactive cysteines SH1 and SH2 with nucleotide binding site closed. The endpoints of cysteine crosslinked energy minimized structure are compared to the native energy minimized structure of myosin S1.

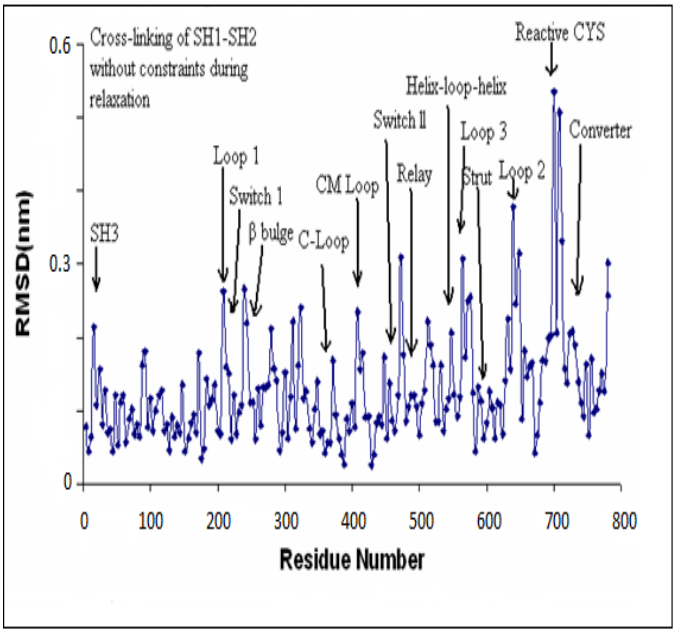

Fig. 1B: Structural changes after simulating the endpoints of energy minimized structure of crosslinkedcysteines with nucleotide binding site closed for 100 ps without constraints during relaxation. The structure obtained after 100 ps of molecular dynamics simulations is compared to the native myosin S1 after 100 ps of stochastic dynamic simulations

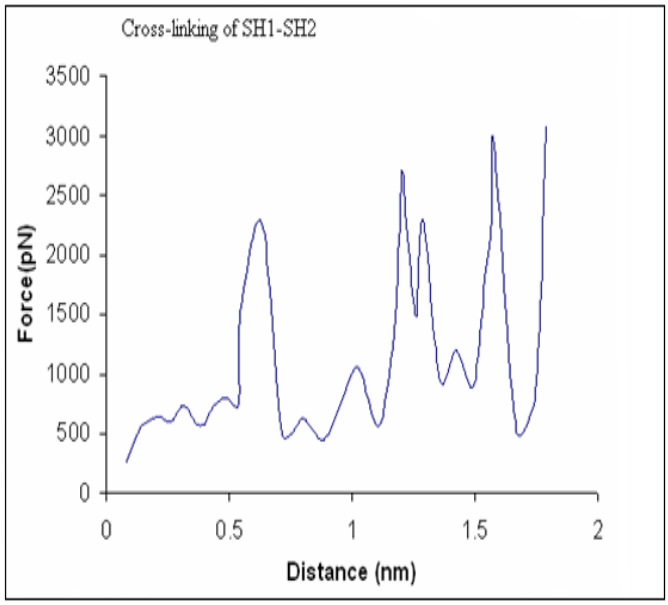

Fig. 1C: Force-distance curve of SH1-SH2 crosslinking with nucleotide binding site closed. Force constraints with a spring constant of 16.7 N/m were used to crosslink the reactive cysteines by changing a distance of 0.1nm decrements followed by energy minimization. The force-distance curve was determined by calculating the difference between the actual distance and the target distance after each energy minimization using the spring constant.

Simulations of the nucleotide binding site

There are no major structural changes in S1 when nucleotide binding site is opened (Fig. 2 A). The single force constraint between residues I182 and S325 induced nucleotide cleft movements that correlated with modest changes throughout the motor domain particularly in the normally flexible regions identified by the dynamics simulations (Fig 2B). With the constraint released from the residue I182 and S325 and dynamics simulations performed for 100 ps there were again modest changes throughout the motor domain particularly in the normally flexible regions. Switch 1, which is not a flexible joint show the highest RMSD. This is because the nucleotide-binding pocket is located at the interface between the N-terminal and 50-kDa upper subdomains, opening of the nucleotide binding pocket causes the rotation of the 50-kDa upper subdomain and that the center of rotation is located in the switch I region which was previously observed experimentally in scallop myosin. Opening of nucleotide site caused little change in the helix leading to the lever arm. If conformational changes from nucleotide site were directly involved in lever arm movement, then the computational opening of the nucleotide site should have affected this helix. Indirect positioning of the lever arm through light chain interactions with the converter region and the SH3 domain seem more consistent

with the simulations. The force-distance plot shows that the opening of the nucleotide site requires the least energy(Fig 2 C).

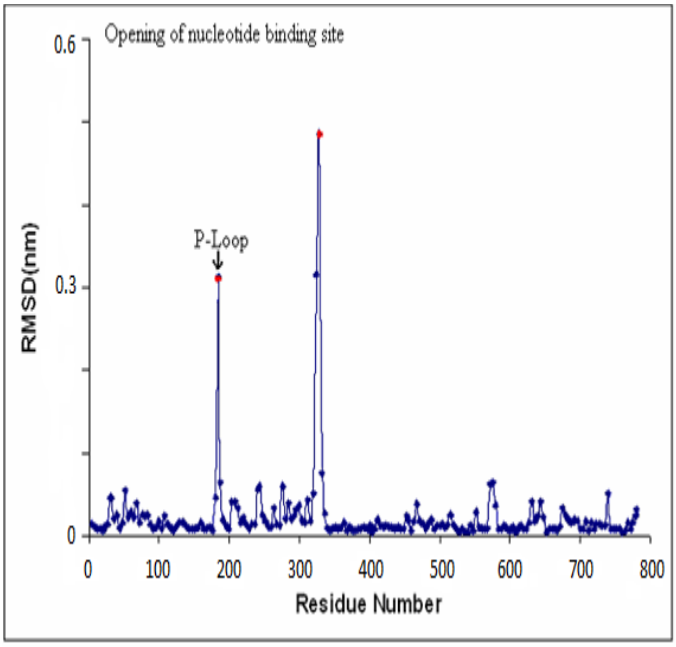

Fig. 2A: Structural changes associated with opening of nucleotide site. The endpoints of energy minimized nucleotide opened site structure are compared to the native energy minimized structure of myosin S1.

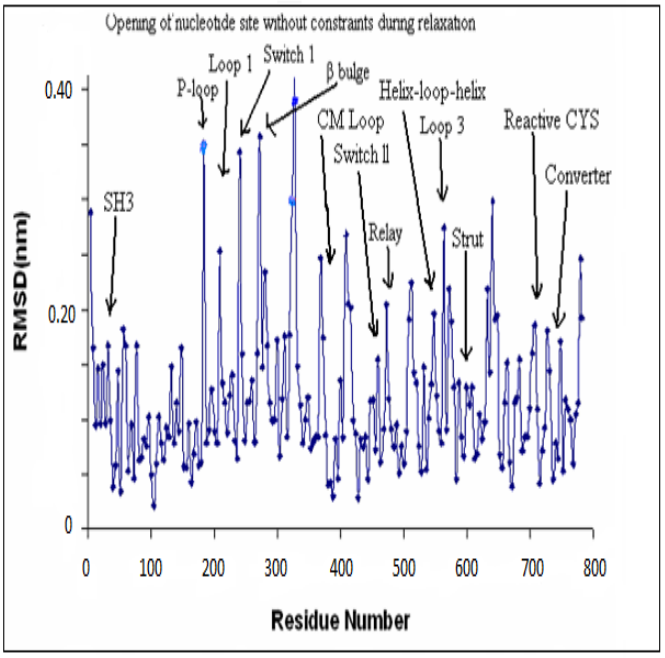

Fig. 2B: Structural changes after simulating the endpoints of energy minimized structure of nucleotide opening site for 100 ps without constraints during relaxation. The structure obtained after 100 ps of molecular dynamics simulations is compared to the native myosin S1 after 100 ps of stochastic dynamic simulations.

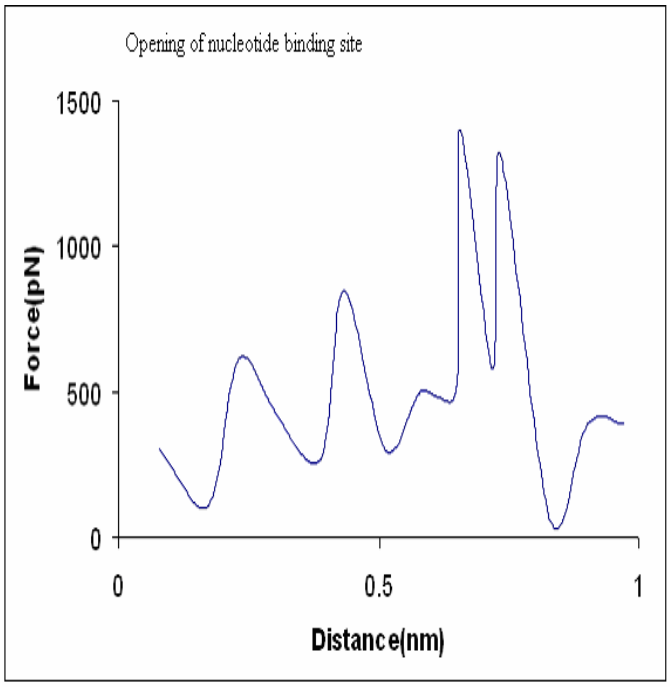

Fig. 2C: Force-distance curve of nucleotide binding site. Force constraints with a spring constant of 16.7 N/m were used to open the nucleotide site SER 180 and SER 324 by changing a distance of 0.1nm increments followed by energy minimization.

Simulations near converter region and nucleotide binding site

When the reactive cysteines are pulled into close proximity after opening nucleotide cleft, alpha-helix that separates the two residues unravels. A number of regions throughout the structure show modest sensitivity to the perturbation even though they are nanometers away from the perturbed site (Fig. 3A) Such peaks in the plot of RMSD correspond to regions of known significance such as loop 1, loop 2, converter region, and the helix between the CM loop, switch 1 and switch 2. The strut which did not show any perturbation during crosslinking the reactive cysteines or opening of the nucleotide cleft shows significant RMSD when forces are applied to the nucleotide cleft in combination with forces applied to the converter region. Crosslinking the reactive cysteines with nucleotide binding site open requires more work than with the nucleotide binding site closed (Fig. 3B). Therefore, with nucleotide binding site closed, the crosslinking is accelerated and the helix undergoes some conformational changes in order for SH1 and SH2 to come close to each other. This could be indicative of helix melting or increased flexibility with nucleotide binding site closed. Previous crosslinking experiments also showed that nucleotides shift the equilibria among conformational states of the helix (Yengo, et al ,2002). This helix appearedalso to be functionally important; the ATPase activity of S1 wasinactivated by its cross-linking (Burkeand Reisler, 1977) and

nucleotides, if present,became non-covalently trapped in the active site (Wells and Yount,1980).

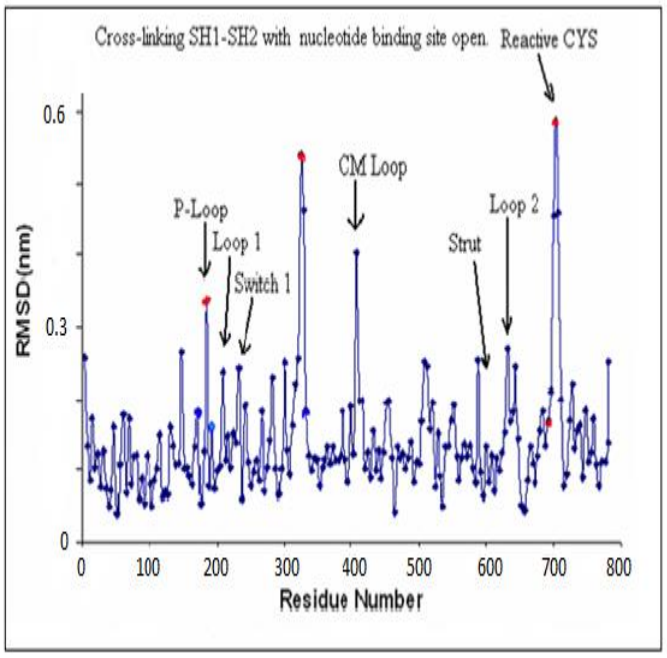

Fig. 3A: Structural changes associated with crosslinking of the reactive cysteines SH1 and SH2 with nucleotide binding site open. The endpoints of cysteine crosslinked energy minimized structure after opening nucleotide binding site is compared to the energy minimized structure of native myosin S1 after 100 ps of molecular dynamics simulations.

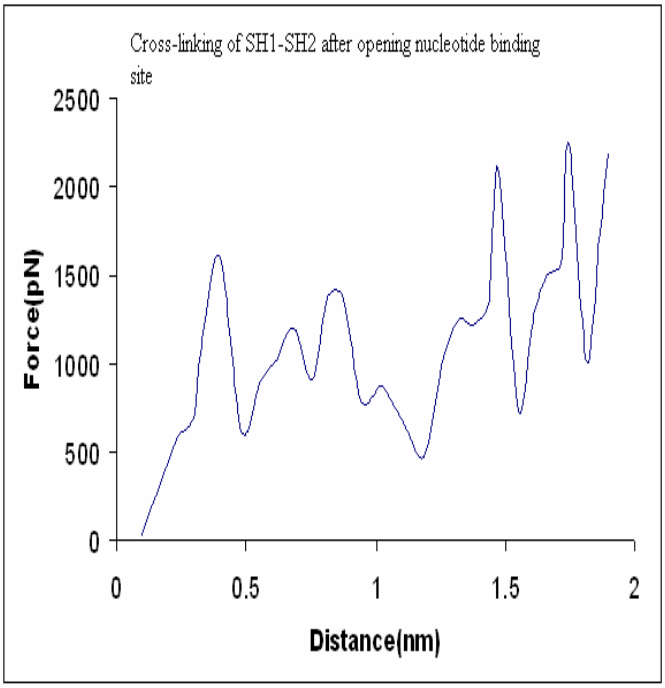

Fig. 3B: Force-distance curve of crosslinking SH1-SH2 after opening nucleotide binding site. Force constraints with a spring constant of 16.7 N/m were used to open the nucleotide site SER 180 and SER 324 by changing a distance of 0.1nm increments followed by energy minimization and then crosslinking SH1-SH2 by changing a distance of 0.1nm increments followed by energy minimization.

Simulations of the 50 kDa cleft and simulations at the converter region

The closing of the 50 kDa cleft structure with crosslinkedcysteines (Fig. 4 A)does not show many

changes when compared to closing the 50 kDa cleft (Fig 5 B). Thestrut gets more rigid when SH1 SH2 iscrosslinked and the RMSD of the strut decreases(Table 2). Whereas, SH3 domain and converter increase in RMSD when the 50 kDa cleftis closed with crosslinkedcysteines. This can be attributed to the constraints at thereactive cysteines. There is not a significant increase in work required to close the 50 kDacleft in presence of crosslinkedcysteines than to close the 50 kDa cleft in absence ofcrosslinkedcysteines (Table. 1).The opening of the 50 kDa cleft structure with crosslinkedcysteines (Fig. 4 B) does not show significant changes when compared to opening the 50 kDa cleft in absence of crosslinkedcysteines (Fig 5 A). The RMSD of the strut decreases on crosslinking but is not significant. The work required to open the cleft after crosslinking the reactive cysteines is less than the work required to open the 50 kDa cleft. The force-distance spectra of opening/closing the cleft in presence of crosslinkedcysteines (Fig. 4C) indicates that the force required to close the cleft is more than it is required to open in the presence of crosslinkedcysteines. The simulations performed for opening/closing the cleft in presence ofcrosslinkedcysteines (Fig 4 A,4 B) indicates that the lower 50 kDa domain shows more flexibility than the upper 50 kDa domain.

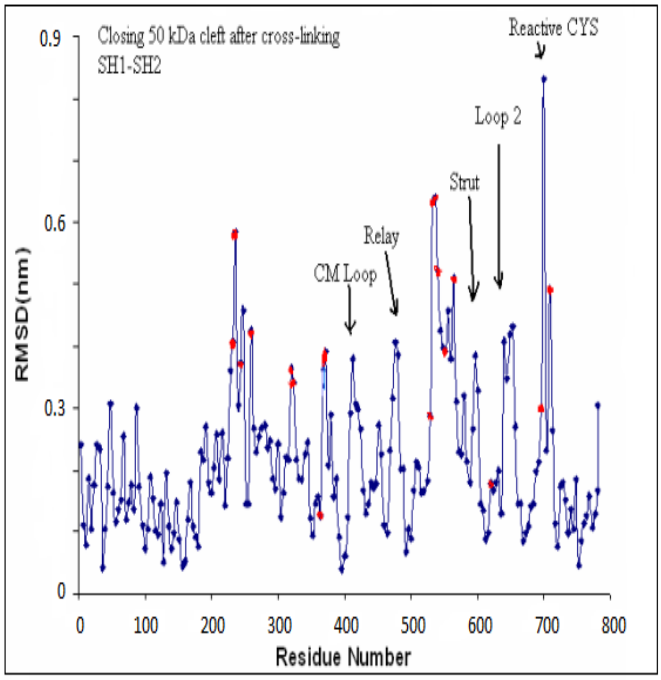

Fig. 4 A: Structural changes associated with closing of the 50kDa cleft after crosslinking the reactive cysteines SH1 and SH2. The endpoints of energy minimized structure are compared to the energy minimized structure of native myosin S1 after 100 ps of molecular dynamics simulations.

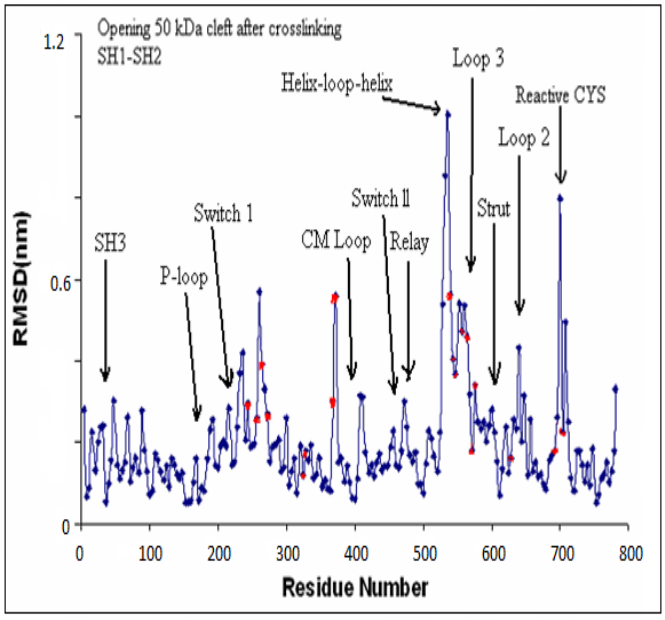

Fig 4 B: Structural changes associated with opening of the 50kDa cleft after crosslinking the reactive cysteines SH1 and SH2. The endpoints of energy minimized structure is compared to the energy minimized structure of native myosin S1 after 100 ps of stochastic dynamic simulations.

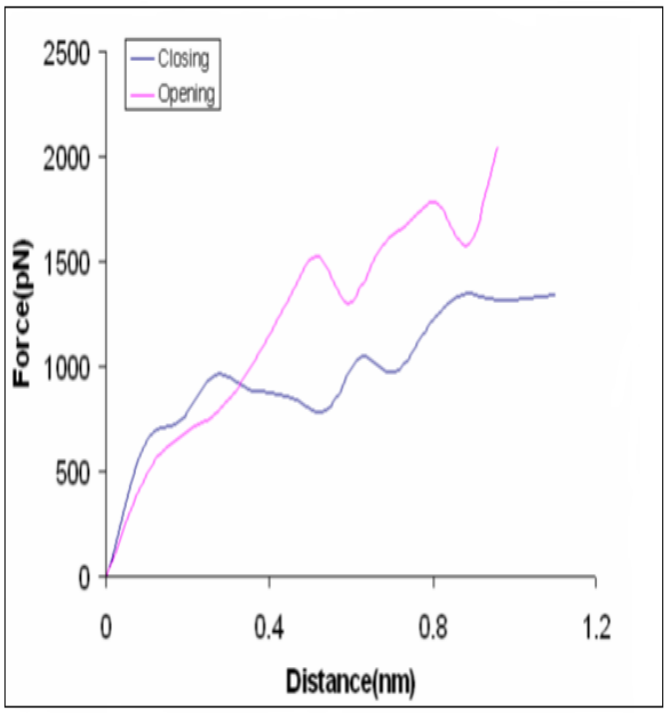

Fig 4C: Simulated closing and opening of the 50 kDa cleft after SH1and SH2 are crosslinked. Force constraints with a spring constant of 16.7 N/m were used to close and open the 50 kDa cleft by changing the target distance at 0.1 nm increments followed by energy minimization. A simulated force–distance curve was calculated based on the difference between the actual distance and the target distance after each energy minimization using the spring constant.

Simulations of the 50 kDa cleft with nucleotide binding site opened

The closing of the 50 kDa cleft structure with nucleotide binding site open (Fig.6 A) does not

show many changes when compared to closing the 50 kDa cleft with nucleotide binding site closed (Fig 5 B). The significant changes are at the converter region and at the reactive cysteines which show an increase in RMSD when the cleft is closed with nucleotide binding site opened. The strut becomes more rigid when 50 kDa cleft is closed with nucleotide binding site opened. The opening of the 50 kDa cleft structure with nucleotide binding site open (Fig. 6 B) does not show many changes when compared to opening the 50 kDa cleft with nucleotide binding site closed (Fig 5 A). The significant changes are at the converter region and at the reactive cysteines which show an increase in RMSD when the 50 kDa cleft is opened with nucleotide binding site opened. The strut becomes more rigid when 50 kDa cleft is opened with nucleotide binding site open. The work required to open the 50 kDa cleft with nucleotide binding site open is more than the work required to open the 50 kDa cleft with nucleotide binding site closed. The work required to open the 50 kDa cleft with nucleotide binding site open is more than the work required to close the cleft with nucleotide binding site open (Table. 1).The simulations of the cleft for opening/closing with nucleotide binding site open indicate that the lower 50 kDa domain shows more flexibility than the upper 50 kDa domain (Fig 6 A, 6 B).

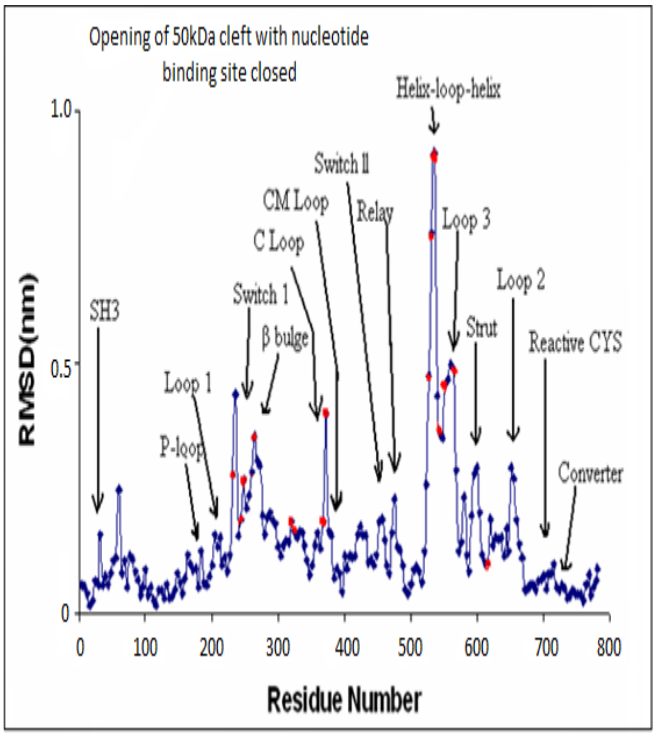

Fig. 5A: Structural changes associated with opening of the 50 kDa cleft with nucleotide binding site closed. The endpoints of energy minimized structure are compared to the native energy minimized structure of myosin S1 and the magnitude of changes is determined from root mean square deviation(RMSD).

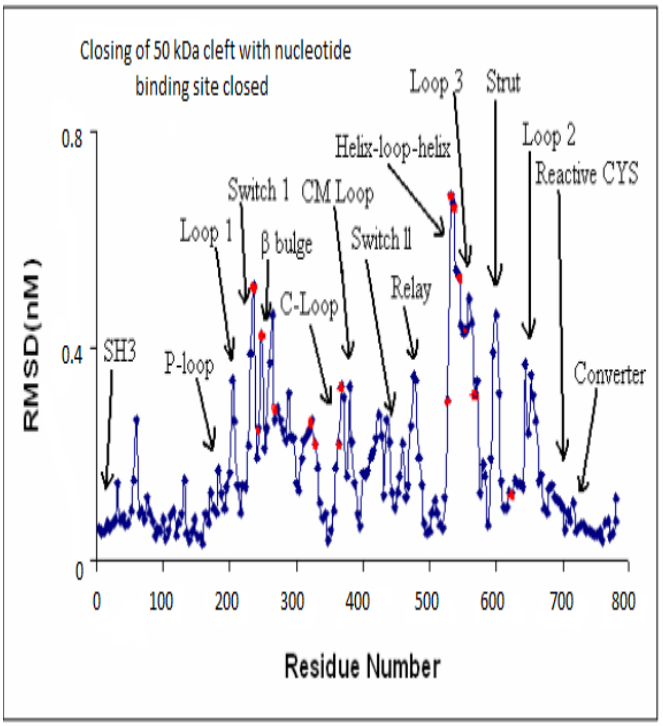

Fig. 5B: Structural changes associated with closing of the 50 kDa cleft with nucleotide binding site closed. The endpoints of energy minimized structure are compared to the native energy minimized structure of myosin S1.

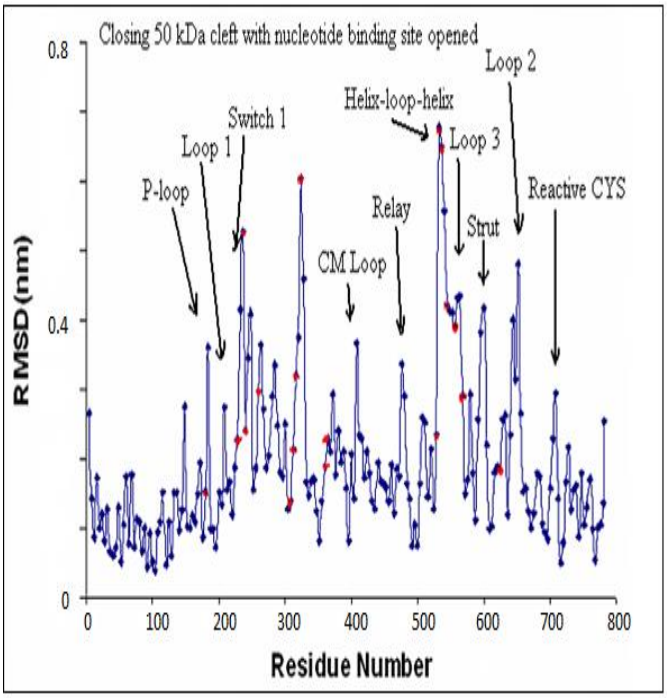

Fig. 6A: Structural changes associated with closing of the 50 kDa cleft after openingnucleotide binding site. The endpoints of energy minimized structure are compared to theenergy minimized structure of native myosin S1 after 100 ps of molecular dynamicssimulations.

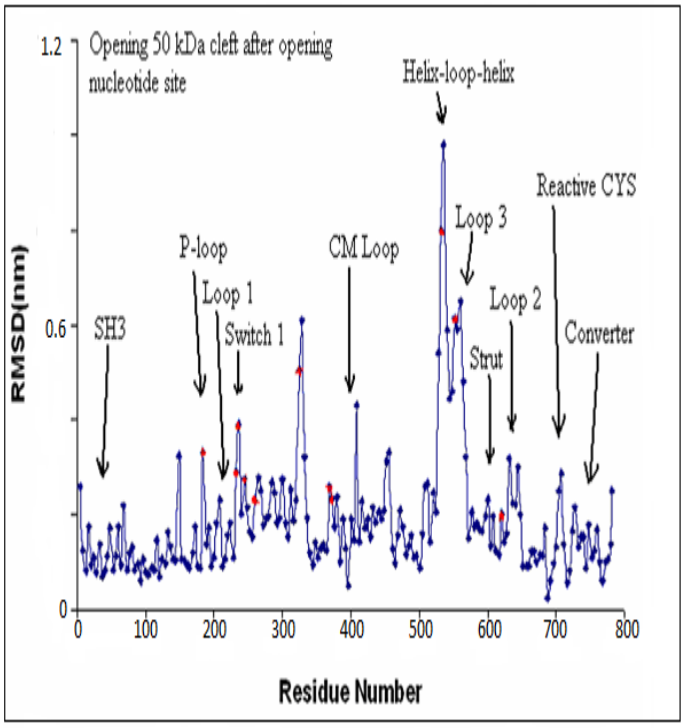

Fig. 6B: Structural changes associated with opening of the 50 kDa cleft after openingthe nucleotide binding site. The endpoints of energy minimized structure are compared tothe energy minimized structure of native myosin S1 after 100 ps of molecular dynamicssimulations.

Simulations of the 50 kDa cleft, nucleotide binding site and simulations at the converter region

The closing of the 50 kDa cleft structure with crosslinkedcysteines andnucleotide binding site opened (Fig. 7 A) does not show many changes whencompared to closing the 50 kDa cleft with nucleotide binding site closed (Fig 5 B). Thesignificant changes are at the converter region and at the reactive cysteines which show an increase in RMSD when the cleft is closed with nucleotide binding site opened. Thestrut becomes more rigid when 50 kDa cleft is closed with crosslinkedcysteines andnucleotide binding site opened but the change is not significant. The work required toclose the 50 kDa cleft with crosslinkedcysteines and nucleotide binding site opened isless than the work required to close the 50 kDa cleft with crosslinkedcysteines andnucleotide binding site closed (Table. 1). The opening of the 50 kDa cleft structure with crosslinkedcysteines and nucleotide binding site opened (Fig. 7 B) does not show significant changes when compared to opening the 50 kDa cleft with nucleotide binding site closed (Fig. 5 A).The significant changes are at the converter region and at the reactive cysteines which show an increase in RMSD when the cleft is closed with nucleotide binding site opened. The strut becomes more rigid when 50 kDa cleft is opened with crosslinkedcysteines and nucleotide binding site opened. The work required to open the

50 kDa cleft with crosslinkedcysteines with nucleotide binding site opened is more than the work required to open the 50 kDa cleft with nucleotide binding site closed (Table. 1). The work required to open the cleft with crosslinkedcysteines and nucleotide binding site opened is more than the work required to close the cleft with crosslinkedcysteines and nucleotide binding site opened (Table. 1).

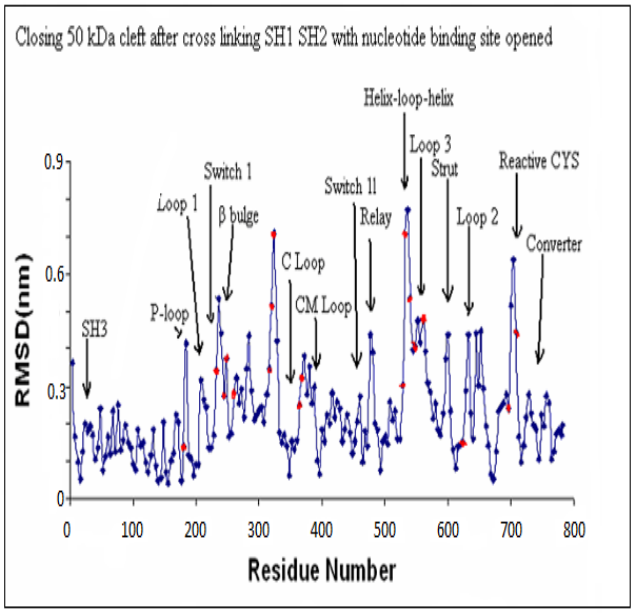

Fig. 7A: Structural changes associated with closing the 50 kDa cleft with cross-linkedcysteines and nucleotide binding site opened. The endpoints of energy minimizedstructure are compared to the energy minimized structure of native myosin S1 after 200 psof molecular dynamics simulations.

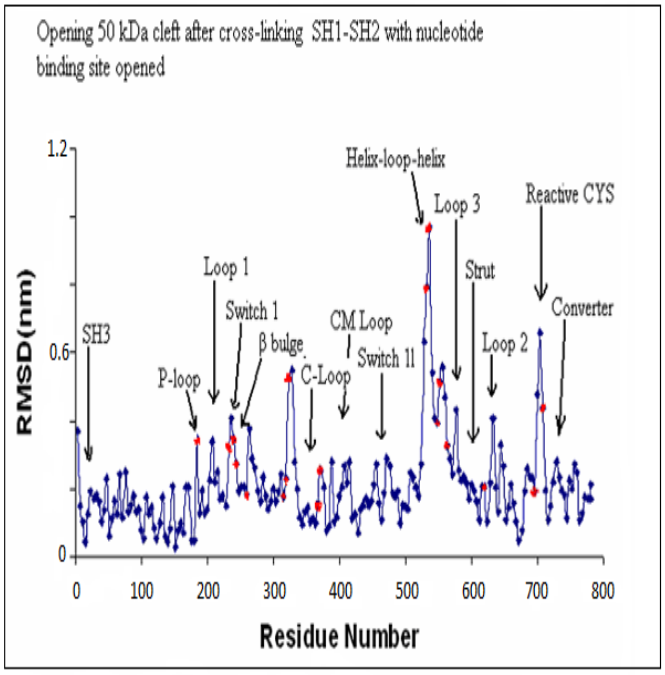

Fig. 7B: Structural changes associated with opening the 50 kDa cleft with cross-linkedcysteines and nucleotide binding site opened. The endpoints of energy minimizedstructure are compared to the energy minimized structure of native myosin S1 after 200 psof molecular dynamics simulations.

Table 1: Amount of work required for various conformational states of myosin.

CONFORMATIONAL STATES OF MYOSIN S1	**WORK (*zepto joules*)**
Opening 50 kDa cleft with nucleotide cleft closed	1038
Closing 50 kDa cleft with nucleotide cleft closed	1102
Opening 50 kDa cleft with nucleotide cleft opened	1147
Closing 50 kDa cleft with nucleotide cleft opened	1104
Opening 50 kDa cleft after crosslinking SH1 SH2 with nucleotide cleft closed	978
Closing 50 kDa cleft after crosslinking SH1 SH2 with nucleotide cleft closed	1133
Opening 50 kDa cleft after crosslinking SH1 SH2 with nucleotide cleft opened	1137
Closing 50 kDa cleft after crosslinking SH1 SH2 with nucleotide cleft opened	972
Crosslinking of SH1 SH2 with nucleotide cleft closed	1733
Crosslinking of SH1 SH2 with nucleotide cleft open	1917
Opening of nucleotide site	427

Based on the results from Table 1, it can be hypothesized that it is easier to open the 50 kDa cleft than close the 50 kDa cleft with nucleotide binding site closed. Whereas, with nucleotide binding site opened it becomes difficult to open the 50 kDa cleft but the closing of the 50 kDa cleft is easier. Cleft closing is independent of the opening or closing of the nucleotide binding site whereas cleft opening is dependent on the nucleotide binding site. Opening the 50 kDa cleft is easier with crosslinked SH1 SH2 and nucleotide binding site

closed .Whereas, closing the 50 kDa cleft becomes difficult with crosslinked SH1 SH2 and nucleotide binding site closed. Crosslinking the reactive cysteines aids in opening the 50 kDa cleft. Opening the 50 kDa cleft is difficult with crosslinked SH1 SH2 and nucleotide binding site opened .Whereas, it becomes easier to close the 50 kDa cleft with crosslinked SH1 SH2 and nucleotide binding site opened. Crosslinking the reactive cysteines makes opening the 50 kDa cleft easier whereas opening of the nucleotide binding site makes it easier to close the 50 kDa cleft.

In summary, the strut which traverses the 50 kDa cleft and plays an important role in positioning the actomyosin binding interface during actin binding and is thought to be intimately linked to distant structural changes in the myosin's nucleotide cleft and neck regions is very rigid. It can be concluded that the strut is more mobile during the closing of 50 kDa cleft with nucleotide binding site closed and the opening of the nucleotide site hardly causes the strut to make any significant movement. Crosslinking of SH1 SH2 with nucleotide cleft open requires maximum energy and opening of nucleotide cleft needs the least amount of energy.

ACKNOWLEDGEMENTS

This work was supported by the National Institute of Arthritis and Musculoskeletal and Skin Diseases of the National Institutes of Health Grant.

REFERENCES

Alberts B, Bray D, Lewis J, Raff M, Roberts K, et al. (1994) Molecular biology of the cell Garland Publishing. 1616 p

D.D. Root, X. Shangguan, J. Xu, M. McAllister, (1999) Determination of Fluorescent Probe Orientations on Biomolecules by Conformational Searching: Algorithm Testing and Applications to the Atomic Model of Myosin, J. Struct. Biol.127, 22-34

Dobbie, I, M. Linari, G. Piazzesi, M. Reconditi, N. Koubassova, M. A. Ferenczi, V. Lombardi, and M. Irving. (1998). Elastic bending and active tilting of myosin heads during

muscle contraction.Nature. 396:383-387.

Douglas. D, and Reisler, E. (1992) Cooperativity of thiol-modified myosin filaments. ATPase and motility assays of myosin function, Biophysical journal 63, 730-740

Eisenberg, E, T. L. Hill, and Y. Chen.(1980). Cross-bridge model of muscle contraction.Biophys. J. 29:195–227

Gao Y, Karplus M (2004) Biomolecular motors: The F_1-ATPase paradigm. CurrOpinStructBiol 14: 250–259

Harford, J, and J. Squire.(1997). Time-resolved diffraction studies of muscle using synchrotron radiation.Rep. Prog. Phys. 60:1723-1787.

Huxley, A. F. (1957). Muscle structure and theories of contraction. Prog.Biophys. 7:255–318.

Huxley, H. E, A. Stewart, H. Sosa, and T. Irving.(1994). X-ray diffraction measurements of the extensibility of actin and myosin filaments in contracting muscle.Biophys. J. 67:2411-2421.

Huxley, H. E. (1996). A personal view of muscle and motility mechanisms.Annu. Rev. Physiol. 58:1-19.

Karplus, M, and McCammon, J. A. (1983) Dynamics of Proteins: Elements and Function Annu. Rev. Biochem. 52, 263-300

Mehta, A. D,Rief, M,Spudich, J. A, Smith, D. A, and Simmons, R. M. (1999) Single-Molecule Biomechanics with Optical Methods Science 283, 1689-1695

Pate, E, and R. Cooke.(1989). A model of cross-bridge action: the effects of ATP, ADP and Pi. J. Muscle Res. Cell Motil. 10:181–196

Radmacher, M, Fritz, M, Hansma, H. G, and Hansma, P. K. (1994) Direct observation of enzyme activity with the atomic force microscope Science 265, 1577-1579

Ravi K.Gawalapu, Douglas D.Root (2006) Fluorescence labeling and computational analysis of the strut of myosin's 50 kDa cleft, Archives of Biochemistry and Biophysics 456,102-111

Rayment, I, H.M. Holden, M. Whittaker, C.B. Yohn, M. Lorenz, K.C. Holmes, and R.A. Milligan.(1993a). Structure of the actin-myosin complex and its implications for muscle contraction.Science. 261: 58-65

Rayment, I,Rypniewski, W. R, Schmidt-Base, K, Smith, R,Tomchick, D. R,Benning, M. M,Winkelmann, D. A,Wesenberg, G, and Holden, H. M. (1993b) Three-dimensional structure of myosin subfragment-1: a molecular motor, Science(New York, N.Y 261, 50-58).

Reisler, E, Burke, M, and Harrington, W. F. (1974) Cooperative role of two sulfhydryl groups in myosin adenosine triphosphatase, Biochemistry 13, 2014-2022.

Sasaki, N,Ohkura, R, and Sutoh, K. (2002) Dictyostelium myosin II as a model to study the actin-myosin interactions during force generation, Journal of muscle research and cell motility 23, 697-702

Takezawa, Y, Kim, D. S,Ogino, M, Sugimoto, Y, Kobayashi, T,Arata, T, and Wakabayashi, K. (1999) Backward Movements of Cross-Bridges by Application of Stretch and by Binding of MgADP to Skeletal Muscle Fibers in the Rigor State as Studied by X-Ray Diffraction Biophys. J. 76, 1770-1783

Todd J. Minehardt,* Nicola Marzari,* Roger Cooke,† Edward Pate,‡ Peter A. Kollman,§ and Roberto Car*(2002) A Classical and Ab Initio Study of the Interaction of the Myosin Triphosphate Binding Domain with

ATP, Biophys J, February 2002, p. 660-675, Vol. 82, No. 2.

Vale RD, Milligan RA (2000) The way things move: Looking under the hood of molecular motor proteins. Science 288: 88–95.

Wakabayashi, K, Y. Sugimoto, H. Tanaka, Y. Ueno, Y. Takezawa, and Y. Amemiya(1994).X-ray diffraction measurements for the extensibility of actin and myosin filaments during muscle contraction.Biophys. J. 67:2422-2435.

Wells, J. A,Knoeber, C, Sheldon, M. C,Werber, M. M, and Yount, R. G. (1980) Cross-linking of myosin subfragment 1. Nucleotide-enhanced modification by a variety of bifunctional reagents, The Journal of biological chemistry 255, 11135-11140.

Yengo, C. M, De La Cruz, E. M,Chrin, L. R, Gaffney, D. P, and Berger, C. L. (2002) Actin-induced closure of the actin-binding cleft of smooth muscle myosin, The Journal of biological chemistry 277, 24114-24119.